



Palmer, KJ., MacCarthy-Morrogh, LJ., Miss Nicola, S., & Stephens, DJ. (2011). A role for Tctex-1 (DYNLT1) in controlling primary cilium length. *European Journal of Cell Biology*, 90(10), 865 - 871.
<https://doi.org/10.1016/j.ejcb.2011.05.003>

Peer reviewed version

Link to published version (if available):
[10.1016/j.ejcb.2011.05.003](https://doi.org/10.1016/j.ejcb.2011.05.003)

[Link to publication record in Explore Bristol Research](#)
PDF-document

NOTICE: this is the author's version of a work that was accepted for publication in the *European Journal of Cell Biology*. Changes resulting from the publishing process, such as peer review, editing, corrections, structural formatting, and other quality control mechanisms may not be reflected in this document. Changes may have been made to this work since it was submitted for publication. A definitive version was subsequently published in *European Journal of Cell Biology*, Volume 90, Issue 10, October 2011, Pages 865–871.

University of Bristol - Explore Bristol Research

General rights

This document is made available in accordance with publisher policies. Please cite only the published version using the reference above. Full terms of use are available:
<http://www.bristol.ac.uk/red/research-policy/pure/user-guides/ebr-terms/>

A role for Tctex-1 (DYNLT1) in controlling primary cilium length.

Krysten J. Palmer, Lucy MacCarthy-Morrogh, Nicola Smyllie, and David J. Stephens *

Cell Biology Laboratories, School of Biochemistry, Medical Sciences Building, University of Bristol,
University Walk, BRISTOL, BS8 1TD, UK

* to whom correspondence should be addressed.

Tel: 00 44 117 331 2173; Fax: 00 44 117 331 2168; Email: david.stephens@bristol.ac.uk

Running title: Tctex-1 controls cilia length.

Keywords: dynein, cilia

Summary

The microtubule motor complex cytoplasmic dynein is known to be involved in multiple processes including endomembrane organization and trafficking, mitosis, and microtubule organization. The majority of studies of cytoplasmic dynein have focussed on the form of the motor that is built around the dynein-1 heavy chain. A second isoform, dynein heavy chain-2, and its specifically associated light intermediate chain, LIC3 (D2LIC), are known to be involved in the formation and function of primary cilia. We have used RNAi in human epithelial cells to define the cytoplasmic dynein subunits that function with dynein heavy chain 2 in primary cilia. We identify the dynein light chain Tctex-1 as a key modulator of cilia length control; depletion of Tctex-1 results in longer cilia as defined by both acetylated tubulin labelling of the axoneme and Rab8a labelling of the cilia membrane. Suppression of dynein heavy chain-2 causes concomitant loss of Tctex-1 and this correlates with an increase in cilia length. Compared to individual depletions, double siRNA depletion of DHC2 and Tctex-1 causes an even greater increase in cilia length. Our data show that Tctex-1 is a key regulator of cilia length and most likely functions as part of dynein-2.

Introduction

Primary cilia are found on nearly all cells in the human body (Satir *et al.*, 2010; Ishikawa and Marshall, 2011). They are a major mechanosensory organelle with key roles in developmental patterning and cell growth control. Dysfunction of primary cilia is associated with a growing number of diseases including polycystic kidney disease and a large array of ciliopathies (Baker and Beales, 2009). The core of the primary cilium is formed by the axoneme, a 9+0 array of microtubules. These microtubules are marked by acetylation allowing specific detection using an antibody to detect this post-translational modification (Piperno and Fuller, 1985). The small GTPase Rab8a has been shown to be required for the formation and function of cilia (Nachury *et al.*, 2007; Yoshimura *et al.*, 2007) and can be used as a marker of the cilia membrane (Hattula *et al.*, 2006) which while contiguous with the rest of the plasma membrane forms a functionally distinct domain. Trafficking with the cilium occurs by intraflagellar transport (Scholey, 2008), a process by which particles are translocated along the axoneme driven by kinesin-2 in the anterograde direction and dynein-2 in the retrograde direction. The particles that are moved are responsible for delivery of components necessary to build and maintain the cilium as well as to remove components and balance the growth of axoneme and membrane.

The microtubule motor cytoplasmic dynein (Paschal *et al.*, 1987; Schroer *et al.*, 1989) has clear roles in microtubule organization, mitosis, organelle structure and positioning, and membrane trafficking (Vallee *et al.*, 2004). In vertebrates, the dynein motor is built around a heavy chain subunit that provides ATPase-dependent force generation as well as microtubule coupling. Associated with this large subunit are a number of accessory subunits that appear to provide some functional specialization of the motor (King *et al.*, 2002). There are two isoforms of the cytoplasmic dynein heavy chain in humans (Gibbons *et al.*, 1994; Vaisberg *et al.*, 1996), DHC1 (DYNC1H1) is the best studied and can be considered the canonical dynein motor responsible for the core functions of dynein. DHC2 (DYNC2H1) (Gibbons *et al.*, 1994) is associated with unique isoforms of

other dynein subunits: an intermediate chain ((FAP133 in *Chlamydomonas reinhardtii*, DYCI-1 in *Caenorhabditis elegans*, and WDR32 in humans (Rompolas *et al.*, 2007; Ishikawa and Marshall, 2011)), a light intermediate chain LIC3 (DYNC2LI1, also called D2LIC) (Grissom *et al.*, 2002; Mikami *et al.*, 2002; Perrone *et al.*, 2003), and light chain LC8 (DYNLL1). Note that throughout we use the common names for the dynein subunits with the gene name as defined by (Pfister *et al.*, 2005) in the first instance of each case. Expression of DHC2 and LIC3 is consistent with a cilia function (Mikami *et al.*, 2002) and compelling evidence exists for a role of these two subunits in the formation and function of primary cilia (Pazour *et al.*, 1998; Pazour *et al.*, 1999; Porter *et al.*, 1999; Signor *et al.*, 1999). Dynein-2 is a principle motor for retrograde intraflagellar transport within the cilium (Scholey, 2008). Notably, cells lacking D2LIC also lack monocilia (Rana *et al.*, 2004) and show defects in embryogenesis. Mutations in DHC2 cause asphyxiating thoracic dystrophy and short rib-polydactyly syndrome, type III (Dagoneau *et al.*, 2009) which are likely also ascribable to defects in cilia. Intriguingly though, in *Tetrahymena thermophila* dynein-2 regulates cilia length but is not itself required for ciliogenesis in (Rajagopalan *et al.*, 2009).

It is intriguing that so little is known of the role for the other subunits of cytoplasmic dynein in the function of dynein-2 or indeed in the process of ciliogenesis or intraflagellar transport. The light chain LC8 has been shown to be involved in this latter process in *Chlamydomonas reinhardtii* (Pazour *et al.*, 1998) and indeed this work provided early compelling evidence of a role for dynein as the principle retrograde motor for intraflagellar transport.

In previous work we have used RNA interference (RNAi) to define the roles of individual subunits of the cytoplasmic dynein motor in intracellular membrane trafficking (Palmer *et al.*, 2009). While previous work has shown that dynein-2 localizes to the Golgi (Grissom *et al.*, 2002), we were unable to define any role for dynein-2 in ER-to-Golgi transport, Golgi organization, recycling endosome function or lysosome distribution (Palmer *et al.*, 2009). During this previous study we used an in vitro assay for the formation of primary cilia (serum starvation of human retinal pigment

epithelial (RPE1) cells and acetylated tubulin labelling of primary cilia) to validate the efficacy of our DHC2 and LIC3 suppression (cited in (Palmer *et al.*, 2009) as unpublished observations). We also used our RNAi approach to determine whether the suppression of other dynein subunits had any effect on primary cilia. Using this approach we found that the suppression of the dynein light chain Tctex-1 caused consistent defects in cilia function, manifest by a dramatic increase in cilia length. This phenotype was indistinguishable from that seen on suppression of DHC2 and indeed further analysis showed that suppression of DHC2 using specific siRNAs caused a concomitant loss of Tctex-1 from cells consistent with a physical interaction. Thus, our data define Tctex-1 as a key regulator of cilia length and implicate it as a component of the dynein-2 motor.

Results and discussion

Our previous work included validation of siRNA duplexes against all known cytoplasmic dynein subunits (Palmer *et al.*, 2009). The majority of this previous work was undertaken in HeLa cells and validated in RPE1. This latter cell line generates primary cilia on serum starvation and consequently we used this to test the requirement for physiological levels of expression of the other dynein subunits in ciliogenesis. Figure 1 shows our validation of the efficacy of dynein-2 suppression in these cells. For all experiments we used suppression of lamin A/C as a siRNA control and α -tubulin as a loading control (shown here for DHC2). Immunoblotting confirmed effective suppression of both DHC1 (Figure 1A) and DHC2 (Figure 1B) in RPE1 cells; expression of DHC2 is weakly detectable with available antibodies making quantification of suppression practically impossible by immunoblotting. Following a total of 72 hours of siRNA suppression including 48 hours of serum starvation, cells were fixed and processed for immunofluorescence using anti-acetylated tubulin as a marker for cilia. It was anticipated from the published literature that DHC2 and LIC3 would show clear phenotypes in this assay (Grissom *et al.*, 2002; Perrone *et al.*, 2003; Rana *et al.*, 2004). The first duplex targeting DHC2 ("DHC2 #1") which was also the most effective as judged by immunoblotting (Figure 1B) and by qPCR (see below and Figure 3C) resulted in a decrease in the number of cells producing cilia. Only 5-15% of "DHC2 #1" transfected cells producing cilia compared to 40-80% in control experiments (n=5 independent experiments, >100 cells). Figure 2A shows cilia in control cells (enlarged in Figure 2B and 2C) with obvious emergence of cilia from centrosomes. Figure 2D (enlarged in Figure 2E-H) shows examples of cilia in DHC2 depleted cells. Cells transfected with DHC2 #1 either have very short cilia (Figure 2E), have normal cilia (Figure 2F, i.e. indistinguishable from control cells), or fail to show cilia (as monitored by elongated acetylated tubulin labelling) (e.g. Figures 2G, H). Suppression of LIC3 yielded similar results (<20% cells producing cilia, data not shown).

Intriguingly cells depleted of DHC2 with a second siRNA duplex, DHC2 #2, showed a distinct phenotype – a clear elongation of cilia (Figure 2J compared to 2I, showing examples of acetylated tubulin-labelling taken at the same magnification from control (lamin A/C suppressed cells, Figure 2I) and DHC2 #2-suppressed cells, Figure 2J). In this case, the number of ciliated cells in each experiment was indistinguishable from controls (ranging from 40-80%). Immunoblotting consistently revealed DHC2 #1 to be most effective at dynein-2 suppression. Our interpretation is that this near-loss of dynein-2 leads to a failure to produce cilia while a partial depletion (as seen using DHC2 #2 for example) led to an increase in cilia length. Cilia elongation on transfection with DHC2 #2 was also validated by imaging GFP-Rab8a labelling of the cilia membrane (Figure 2K).

Previous work has shown localization of dynein-2 to the Golgi apparatus (Grissom *et al.*, 2002). We therefore tested its role in Golgi organization. Figure 2L shows that the Golgi apparatus (marked by giantin labelling) is unaffected by DHC2 suppression (siRNA #2 shown, indistinguishable results were found using siRNA #1). Quantification of multiple images from 5 independent experiments revealed no statistically detectable difference in number, size or distribution of giantin-labelled Golgi structures suggesting that dynein-2 is not required for the structural organization of this organelle (see also (Palmer *et al.*, 2009)).

Following on from this, we decided to test all cytoplasmic dynein subunits for their role in ciliogenesis in these cells. Cells were transfected with validated siRNA duplexes targeting each subunit individually (Palmer *et al.*, 2009). We then used automated detection and measurement of the ciliary axoneme in cells suppressed for each cytoplasmic dynein subunit. Figure 3A shows the results from these assays (n=3) for those dynein subunits for which a phenotype was evident (and statistically validated). Statistically detectable increases in cilia length were seen following suppression of Tctex-1. Only one of two of our siRNA duplexes targeting LC8 produced an increase in cilia length in this assay despite clear evidence of a role for LC8 in cilia (Pazour *et al.*, 1998). Many cells did show a clear increase in cilia length on suppression using the LC8-1 duplex but this

was not statistically detectable following automated image quantification. In contrast, both duplexes targeting Tctex-1 showed a consistent increase in cilia length (Figure 3A). Individual data points are plotted in Figure 3B along with the mean values (grey bars). Suppression of other dynein subunits (DHC1 (DYNC1H1), IC2 (DYNC1I2), LIC1 (DYNC1LI1), LIC2 (DYNC1LI2), or most notably the other light chains rp3 (DYNLT3) or Roadblock-1 (DYNLRB)) resulted in no difference in cilia length when compared to either non-transfected, or lamin A/C suppressed cells (not shown).

To resolve the discrepancy between the data following suppression using DHC2 #1 and DHC2 #2, we used a further 3 siRNA duplexes targeting DHC2. Figure 3A and 3B show that these duplexes (DHC2 #3, #4, and #5) all led to a statistically detectable increase in cilia length. As with DHC2 #2, the number of ciliated cells was the same as in control experiments. These data correlated well with the efficacy of knockdown as measured using quantitative PCR (Figure 3C). Our interpretation is that highly effective suppression of DHC2 (by DHC2 #1) leads to a failure to produce cilia in hTERT-RPE-1 cells where partial suppression (using DHC2 #2, #3, #4, or #5) result in increased cilia length.

Suppression of Tctex-1 was validated using immunoblotting (Figure 3D). In addition to measuring the length of the axoneme, we transfected cells suppressed for Tctex-1 with GFP-Rab8a to determine the length of the cilium membrane. We observed an increase in length of the cilia membrane in cells depleted of Tctex-1 compared to controls (Figure 3E). The data from these experiments gave the same results as those in which we measured axoneme length (data not shown).

To examine the relationship between DHC2 and Tctex-1, we immunoblotted cell lysates following suppression of DHC2 to determine the stability of Tctex-1 (Figure 4A). To our surprise, we noted that the 4 siRNA duplexes targeting DHC2 that produced an increase in the length of the axoneme resulted in loss of Tctex-1 (Figure 4B, grey bars). That we see this with four independent sequences

argues strongly against an off target effect. It is not entirely clear why we do not observe a loss of Tctex-1 following suppression using the DHC2 #1 duplex but one possibility is that this reflects some adaptation of the cells during the 72 hour time course of these experiments. Double transfection with DHC2 #1 and Tctex-1 #1 resulted in a failure of >95% (n=3 independent experiments, total 200 cells) of cells to produce cilia (Figure 4C). These data reflect those seen following depletion of DHC2 alone. Depletion with both DHC2 #2 and Tctex-1 #2 resulted in an increase in cilia length over and above that seen with single depletions alone (Figure 4C). Here the mean cilium length was 4.2 μ m, compared to 1.8 μ m for lamin A/C siRNA, 2.7 μ m for Tctex-1 siRNA #2, and 2.5 μ m for DHC2 siRNA #2. This more robust phenotype is consistent with Tctex-1 and DHC2 acting in the same complex.

We conclude from this that Tctex-1 is a component of dynein-2 that is specifically required for the control of elongation of primary cilia. Despite extensive efforts we have been unable to demonstrate biochemically that Tctex-1 is indeed associated with DHC2 as well as DHC1 (robust association with DHC1 is readily detectable, not shown). The availability of antibodies that are capable of discriminating between the closely related dynein heavy chains is a major limitation here. A major caveat here is that available reagents might preclude detection of any interaction but our data would also be consistent with a dynein-2 independent function for Tctex-1 in regulating cilia length. However, we believe this unlikely for the following reasons. In *Chlamydomonas*, dynein-2 is known to include LIC3 and functional data strongly implicate LC8 in this complex (Pazour *et al.*, 1998; Cole, 2003; Perrone *et al.*, 2003). While LIC3 and DHC2 co-immunoprecipitate together LC8 did not co-sediment or co-immunoprecipitate with DHC2 (Perrone *et al.*, 2003). This is consistent with the many dynein-independent functions of LC8 (King, 2008). Tctex1 and rp3 are capable of forming heterodimers (Lo *et al.*, 2007) but only homodimeric complexes of either Tctex-1 or rp3 are capable of binding to dynein intermediate chains (Lo *et al.*, 2007). Conflicting data exist relating to dynein-independent functions of Tctex-1. Sucrose density centrifugation showed that all Tctex-1 was found

in fractions that co-sediment with the intact dynein complex (Lo *et al.*, 2007), suggesting that unlike for LC8 (King, 2008), all Tctex-1 is in a dynein-based complex. However, other work has identified dynein-independent pools of Tctex-1 (Tai *et al.*, 1998) and suggested dynein-independent functions for Tctex-1 in neurite outgrowth (Chuang *et al.*, 2005). Reconciliation of these data might come from the observation that the association of Tctex-1 with dynein is controlled by protein phosphorylation (Yeh *et al.*, 2006). Indeed a picture appears to be emerging of functions for Tctex-1 following its regulated dissociation from the dynein complex. Intriguingly, these appear to include the regulation of cilium disassembly as cells re-enter mitosis following a period in Go (Li *et al.*, 2011). Together these data are consistent with a model in which Tctex-1 is found in the context of both dynein-1 and dynein-2 complexes. We believe that the simplest interpretation of our own data is that Tctex-1 is a component of dynein-2 that is required for length control in primary cilia. Whether its regulated dissociation from dynein-2 is selectively involved in ciliary disassembly (Li *et al.*, 2011) remains to be tested. It is important to note here that siRNA depletion of Tctex-1 is of course not the same as its regulated dissociation from dynein. Li *et al.* (2001) propose a model in which phosphorylated Tctex-1 (independent of dynein) has a direct role in regulating actin dynamics around the centrosomes to trigger breakdown of the cilium. Clearly, in Tctex-1 depleted cells, such a mechanism would not occur.

In several systems, it has been clearly demonstrated that loss of dynein-2 function results in short cilia that are enlarged with electron dense material, likely due to defects in retrograde IFT (Pazour *et al.*, 1999; Porter *et al.*, 1999; Rana *et al.*, 2004). Our data show that effective suppression of DHC2 results in a loss of cilia formation in cells. We do observe an increase in the number of shortened cilia but also frequently classify cells as non-ciliated (i.e. they have no acetylated tubulin labelling that extends beyond the centrosome).

Why then does partial loss of DHC2 function, or suppression of Tctex-1 lead to lengthening of cilia on our system? In single celled organisms and mammals, significant data exists that implicates IFT

directly in the control of cilium length (Iomini *et al.*, 2001; Engel *et al.*, 2009; Besschetnova *et al.*, 2010). It is intriguing to consider these data in the light of what has been observed in *Tetrahymena* where knockout of dynein-2 function does not result in loss of cilia but instead in a loss of cilia length control (Rajagopalan *et al.*, 2009). This is clearly a very different experimental system, and notably a knockout versus a knockdown. However, it raises the possibility that a disturbance of normal dynein-2 function in these two systems might reflect a similar outcome in the role of IFT in axoneme lengthening. During IFT, the kinesin-2 motor actively delivers dynein-2 to the tip of the cilium to initiate retrograde transport (reviewed in (Scholey, 2008)). In mammalian dynein-2 knockouts (Rana *et al.*, 2004), the accumulation of anterograde IFT particles leads to stumpy cilia. Perhaps in our dynein-2 knockdowns, partial inhibition of retrograde IFT does not lead to a failure of anterograde IFT and so cilia length increases. Consistent with this idea, anterograde IFT is ongoing in *C. elegans* DHC2 mutants, (Signor *et al.*, 1999). Why this is also seen in *Tetrahymena* dynein-2 knockouts (Rajagopalan *et al.*, 2009) is unclear. Perhaps kinesin-2 activity in *Tetrahymena* does is not controlled by the presence of dynein-2.

One possible model arising from this would be that the presence of dynein-2 is required to engage kinesin-2 activity for anterograde IFT. In our knockdowns, we do not lose sufficient dynein-2 to prevent this but do have significant effects on retrograde transport, thus, cilia length increases. Perhaps this is phenocopied by loss of Tctex-1 because Tctex-1 is required for retrograde IFT but not control of kinesin-2 activity. Tctex-1 might directly engage a specific cargo during IFT that is intimately involved in length control through intracellular signalling (Besschetnova *et al.*, 2010) or through control of IFT particle size (Engel *et al.*, 2009). In summary, our data reveal a role for Tctex-1 in controlling the length of primary cilia in human cells. The exact role of Tctex-1 whether in cargo binding, communication with other motors, or intracellular signalling awaits further study.

Materials and Methods

All reagents were purchased from Sigma-Aldrich (Poole, UK) unless stated otherwise. GFP-Rab8a (Hattula *et al.*, 2006) was a kind gift from Johan Peränen (Helsinki, Finland) and was transfected 24 hours prior to imaging or fixation. Antibody sources were as follows: anti-alpha tubulin (Clone DM1A) was from Sigma-Aldrich, anti-acetylated tubulin (Sigma-Aldrich, Poole UK; clone 6-11B-1 (Piperno and Fuller, 1985)), anti-giantin (rabbit polyclonal, Covance, Princeton, New Jersey), DHC2 and LIC3 antibodies were kind gifts from Prof Richard McIntosh (Boulder, CO), Stephen J King (University of Missouri-Kansas City) and Richard Vallee (Columbia University, New York). Anti-Tctex-1 was kindly provided by Viki Allan (University of Manchester, UK). An additional anti-Tctex-1 was purchased from Santa Cruz Biotechnology (Santa Cruz, CA). Horseradish peroxidase conjugated anti-GAPDH and anti-lamin A/C were from Cell Signaling Technologies/NEB (Hitchin, UK).

siRNA transfection and quantitative PCR.

Human telomerase immortalized retinal pigment epithelial cells (hTERT-RPE1) were depleted of targets using siRNA. Key siRNA sequences were as follows (DHC2 #1, DHC2 #2, Tctex-1 #1, and Tctex-1 #2 were previously used in (Palmer *et al.*, 2009). Duplexes were designed to target all known splice variants of each subunit by searching the NCBI database (October 2005). Duplexes were designed using the online tool of Eurofins MWG Operon (Ebersberg, Germany) and synthesized with dTdT overhangs. Duplexes were transfected using a modified calcium phosphate method at 3% CO₂ as described previously (Watson and Stephens, 2006). In all cases, cells were used for experiments 72 h after transfection. Cells were serum starved for the final 48 hours of depletion before either live cell imaging or methanol fixation and immunofluorescence.

DHC2 #1: GGA AUU GAA UAC UCU UCA A; DHC2 #2: ACA GGC UCU UCU CUC UGA A ; DHC2
#3: GCA GUG CAC UUA UUC AAG A; DHC2 #4: GUC UGA AGA UAA CAU AUG A; DHC2
#5:UCA GUA GAA UCU AAU GAC A.

DYNLT1 #1: AUA CAU CGU GAC CUG UGU A; DYNLT1 #2: GUG AAC CAG UGG ACC ACA A

Sequences of all other siRNA oligonucleotides (MWG-Eurofins) along with details of the siRNA
screening platform and image acquisition and processing have been previously described (Palmer
et al., 2009).

Quantitative PCR was performed as described previously (Palmer *et al.*, 2009). Briefly, RNA was
isolated from cells using the TRIzol extraction method (Invitrogen, Paisley, UK). 50 µg RNA was
used for reverse transcription using Omniscript reverse transcriptase (Qiagen, Crawley, United
Kingdom) for 60 min at 37°C. Newly synthesized cDNA was then used for real-time qPCR using the
DyNAmo SYBR green qPCR kit (New England Biolabs, Ipswich, MA). The following primers were
used (designed using Primer3 software; (Rozen and Skaletsky, 2000); available at
<http://primer3.wiki.sourceforge.net>). Primers used were designed using Primer3 software. Two sets
of primers were designed against DHC2 and gave indistinguishable results. The primer pairs (5'-3')
used were: (fwd) TTG GAC TTC CTA GGG GGA CT with (rev) CTC CAA CTC CCC AAA GAT CA
and (fwd) ACA GCT AGC CAA GCT CGA AG with (rev) GAT AGG CAT CCC GTT CTT GA. Each
sample was run in triplicate using the target primers, together with primers designed to amplify RNA
polymerase II (fwd, GCACCACGTCCAATGACAT and rev, GTGCGGCTGCTTCCATAA), as a
control. Amplification was performed and detected using an Opticon2 cycler (Bio-Rad, Hercules,
CA), and data were analyzed using the comparative Ct method, which utilizes the formula $2^{(-\Delta\Delta CT)}$,
where Ct is regarded as the threshold cycle). The amount of target relative to lamin A/C–
suppressed samples and normalized to RNA polymerase II was calculated.

279 **Quantification of image data and statistical analysis**

280 Cilia length was measured using automated detection of acetylated tubulin labelling and the
281 measurement functions in Volocity (version 4.3, Perkin-Elmer, Seer Green, UK). Statistical
282 differences between two groups of data were analysed using ANOVA with a Dunnett's post-hoc
283 multiple comparison test (each condition relative to lamin A/C suppression) in GraphPad Prism 4
284 (GraphPad Software, Inc., La Jolla, CA).

Acknowledgments

We are very grateful to Jon Lane and members of the Stephens lab for helpful discussions and critical input to the manuscript. We are especially grateful to Richard McIntosh, Stephen King, Richard Vallee, Johan Peränen, and Viki Allan for reagents and to the reviewers for their insight and suggestions. This work was funded by a Non-Clinical Senior Research Fellowship (to DJS) and the University of Bristol.

- 293 Baker, K., and Beales, P.L., 2009. Making sense of cilia in disease: the human ciliopathies. *Am J*
294 *Med Genet C* 151C, 281-295.
- 295 Besschetnova, T.Y., Kolpakova-Hart, E., Guan, Y., Zhou, J., Olsen, B.R., and Shah, J.V., 2010.
296 Identification of signaling pathways regulating primary cilium length and flow-mediated adaptation.
297 *Curr. Biol.* 20, 182-187.
- 298 Chuang, J.Z., Yeh, T.Y., Bollati, F., Conde, C., Canavosio, F., Caceres, A., and Sung, C.H., 2005.
299 The dynein light chain Tctex-1 has a dynein-independent role in actin remodeling during neurite
300 outgrowth. *Dev. Cell* 9, 75-86.
- 301 Cole, D.G., 2003. The intraflagellar transport machinery of *Chlamydomonas reinhardtii*. *Traffic* 4,
302 435-442.
- 303 Dagoneau, N., Goulet, M., Genevieve, D., Sznajder, Y., Martinovic, J., Smithson, S., Huber, C.,
304 Baujat, G., Flori, E., Tecco, L., Cavalcanti, D., Delezoide, A.L., Serre, V., Le Merrer, M., Munnich,
305 A., and Cormier-Daire, V., 2009. DYNC2H1 mutations cause asphyxiating thoracic dystrophy and
306 short rib-polydactyly syndrome, type III. *Am. J. Hum. Genet.* 84, 706-711.
- 307 Engel, B.D., Ludington, W.B., and Marshall, W.F., 2009. Intraflagellar transport particle size scales
308 inversely with flagellar length: revisiting the balance-point length control model. *J. Cell Biol.* 187, 81-
309 89.
- 310 Gibbons, B.H., Asai, D.J., Tang, W.J., Hays, T.S., and Gibbons, I.R., 1994. Phylogeny and
311 expression of axonemal and cytoplasmic dynein genes in sea urchins. *Mol. Biol. Cell* 5, 57-70.
- 312 Grissom, P.M., Vaisberg, E.A., and McIntosh, J.R., 2002. Identification of a novel light intermediate
313 chain (D2LIC) for mammalian cytoplasmic dynein 2. *Mol. Biol. Cell* 13, 817-829.
- 314 Hattula, K., Furuholm, J., Tikkanen, J., Tanhuanpää, K., Laakkonen, P., and Peranen, J., 2006.
315 Characterization of the Rab8-specific membrane traffic route linked to protrusion formation. *J. Cell*
316 *Sci.* 119, 4866-4877.
- 317 Iomini, C., Babaev-Khaimov, V., Sassaroli, M., and Piperno, G., 2001. Protein particles in
318 *Chlamydomonas* flagella undergo a transport cycle consisting of four phases. *J. Cell Biol.* 153, 13-
319 24.
- 320 Ishikawa, H., and Marshall, W.F., 2011. Ciliogenesis: building the cell's antenna. *Nat Rev Mol Cell*
321 *Biol* 12, 222-234.
- 322 King, S.J., Bonilla, M., Rodgers, M.E., and Schroer, T.A., 2002. Subunit organization in cytoplasmic
323 dynein subcomplexes. *Protein Sci.* 11, 1239-1250.
- 324 King, S.M., 2008. Dynein-independent functions of DYNLL1/LC8: redox state sensing and
325 transcriptional control. *Sci Signal* 1, pe51.
- 326 Li, A., Saito, M., Chuang, J.Z., Tseng, Y.Y., Dedesma, C., Tomizawa, K., Kaitsuka, T., and Sung,
327 C.H., 2011. Ciliary transition zone activation of phosphorylated Tctex-1 controls ciliary resorption, S-
328 phase entry and fate of neural progenitors. *Nat. Cell Biol.*
- 329 Lo, K.W., Kogoy, J.M., Rasoul, B.A., King, S.M., and Pfister, K.K., 2007. Interaction of the DYNLT
330 (TCTEX1/RP3) light chains and the intermediate chains reveals novel intersubunit regulation during
331 assembly of the dynein complex. *J. Biol. Chem.* 282, 36871-36878.

332 Mikami, A., Tynan, S.H., Hama, T., Luby-Phelps, K., Saito, T., Crandall, J.E., Besharse, J.C., and
 333 Vallee, R.B., 2002. Molecular structure of cytoplasmic dynein 2 and its distribution in neuronal and
 334 ciliated cells. *J. Cell Sci.* 115, 4801-4808.

335 Nachury, M.V., Loktev, A.V., Zhang, Q., Westlake, C.J., Peranen, J., Merdes, A., Slusarski, D.C.,
 336 Scheller, R.H., Bazan, J.F., Sheffield, V.C., and Jackson, P.K., 2007. A core complex of BBS
 337 proteins cooperates with the GTPase Rab8 to promote ciliary membrane biogenesis. *Cell* 129,
 338 1201-1213.

339 Palmer, K.J., Hughes, H., and Stephens, D.J., 2009. Specificity of cytoplasmic dynein subunits in
 340 discrete membrane-trafficking steps. *Mol. Biol. Cell* 20, 2885-2899.

341 Paschal, B.M., Shpetner, H.S., and Vallee, R.B., 1987. MAP 1C is a microtubule-activated ATPase
 342 which translocates microtubules in vitro and has dynein-like properties. *J. Cell Biol.* 105, 1273-1282.

343 Pazour, G.J., Dickert, B.L., and Witman, G.B., 1999. The DHC1b (DHC2) isoform of cytoplasmic
 344 dynein is required for flagellar assembly. *J. Cell Biol.* 144, 473-481.

345 Pazour, G.J., Wilkerson, C.G., and Witman, G.B., 1998. A dynein light chain is essential for the
 346 retrograde particle movement of intraflagellar transport (IFT). *J. Cell Biol.* 141, 979-992.

347 Perrone, C.A., Tritschler, D., Taulman, P., Bower, R., Yoder, B.K., and Porter, M.E., 2003. A novel
 348 dynein light intermediate chain colocalizes with the retrograde motor for intraflagellar transport at
 349 sites of axoneme assembly in chlamydomonas and Mammalian cells. *Mol. Biol. Cell* 14, 2041-2056.

350 Pfister, K.K., Fisher, E.M., Gibbons, I.R., Hays, T.S., Holzbaur, E.L., McIntosh, J.R., Porter, M.E.,
 351 Schroer, T.A., Vaughan, K.T., Witman, G.B., King, S.M., and Vallee, R.B., 2005. Cytoplasmic
 352 dynein nomenclature. *J. Cell Biol.* 171, 411-413.

353 Piperno, G., and Fuller, M.T., 1985. Monoclonal antibodies specific for an acetylated form of alpha-
 354 tubulin recognize the antigen in cilia and flagella from a variety of organisms. *J. Cell Biol.* 101,
 355 2085-2094.

356 Porter, M.E., Bower, R., Knott, J.A., Byrd, P., and Dentler, W., 1999. Cytoplasmic dynein heavy
 357 chain 1b is required for flagellar assembly in Chlamydomonas. *Mol. Biol. Cell* 10, 693-712.

358 Rajagopalan, V., Subramanian, A., Wilkes, D.E., Pennock, D.G., and Asai, D.J., 2009. Dynein-2
 359 affects the regulation of ciliary length but is not required for ciliogenesis in Tetrahymena
 360 thermophila. *Mol. Biol. Cell* 20, 708-720.

361 Rana, A.A., Barbera, J.P., Rodriguez, T.A., Lynch, D., Hirst, E., Smith, J.C., and Beddington, R.S.,
 362 2004. Targeted deletion of the novel cytoplasmic dynein mD2LIC disrupts the embryonic organiser,
 363 formation of the body axes and specification of ventral cell fates. *Development* 131, 4999-5007.

364 Rompolas, P., Pedersen, L.B., Patel-King, R.S., and King, S.M., 2007. Chlamydomonas FAP133 is
 365 a dynein intermediate chain associated with the retrograde intraflagellar transport motor. *J. Cell Sci.*
 366 120, 3653-3665.

367 Rozen, S., and Skaletsky, H., 2000. Primer3 on the WWW for general users and for biologist
 368 programmers. *Methods Mol. Biol.* 132, 365-386.

369 Satir, P., Pedersen, L.B., and Christensen, S.T., 2010. The primary cilium at a glance. *J. Cell Sci.*
 370 123, 499-503.

371 Scholey, J.M., 2008. Intraflagellar transport motors in cilia: moving along the cell's antenna. *J. Cell*
 372 *Biol.* 180, 23-29.

373 Schroer, T.A., Steuer, E.R., and Sheetz, M.P., 1989. Cytoplasmic dynein is a minus end-directed
 374 motor for membranous organelles. *Cell* 56, 937-946.

375 Signor, D., Wedaman, K.P., Orozco, J.T., Dwyer, N.D., Bargmann, C.I., Rose, L.S., and Scholey,
 376 J.M., 1999. Role of a class DHC1b dynein in retrograde transport of IFT motors and IFT raft
 377 particles along cilia, but not dendrites, in chemosensory neurons of living *Caenorhabditis elegans*.
 378 *J. Cell Biol.* 147, 519-530.

379 Tai, A.W., Chuang, J.Z., and Sung, C.H., 1998. Localization of Tctex-1, a cytoplasmic dynein light
 380 chain, to the Golgi apparatus and evidence for dynein complex heterogeneity. *J. Biol. Chem.* 273,
 381 19639-19649.

382 Vaisberg, E.A., Grissom, P.M., and McIntosh, J.R., 1996. Mammalian cells express three distinct
 383 dynein heavy chains that are localized to different cytoplasmic organelles. *J. Cell Biol.* 133, 831-
 384 842.

385 Vallee, R.B., Williams, J.C., Varma, D., and Barnhart, L.E., 2004. Dynein: An ancient motor protein
 386 involved in multiple modes of transport. *J. Neurobiol.* 58, 189-200.

387 Yeh, T.Y., Peretti, D., Chuang, J.Z., Rodriguez-Boulan, E., and Sung, C.H., 2006. Regulatory
 388 dissociation of Tctex-1 light chain from dynein complex is essential for the apical delivery of
 389 rhodopsin. *Traffic* 7, 1495-1502.

390 Yoshimura, S., Egerer, J., Fuchs, E., Haas, A.K., and Barr, F.A., 2007. Functional dissection of Rab
 391 GTPases involved in primary cilium formation. *J. Cell Biol.* 178, 363-369.

392
 393

Figure Legends:

Figure 1: Suppression of dynein heavy chains in RPE1 cells. Cells were transfected with siRNA duplexes targeting either DHC1 or DHC2 or lamin A/C as a positive control. 72 hours after transfection, cell lysates were separated by SDS-PAGE on 5% gels and immunoblotted for either (A) DHC1 or (B) DHC2. Lamin A/C and α -tubulin are included as siRNA and loading controls respectively (tubulin loading control shown for one example only). Molecular weight markers as indicated by arrows.

Figure 2: Depletion of DHC2 results in increase cilia length. (A, B) Cells transfected with siRNA targeting (A) lamin A/C or (B) DHC2 #1 were labelled to detect acetylated tubulin. Insets (B) and (C) show cilia in control cells; DHC2 depletion with duplex #1 results in either very short cilia (D), some normal cilia (F) and many cells with no acetylated tubulin labelling visibly extending beyond the centrosome (scored as no cilia, G, H). (I, J) depletion of DHC2 with siRNA#2 results in elongated cilia (J) compared to controls (I); five examples of each are shown. (K) Cilia elongation following transfection with DHC2 siRNA #2 is also evident when using GFP-Rab8a as a marker for the cilium membrane. (L) Cells were labelled to detect giantin (Golgi apparatus) and acetylated tubulin (axoneme and centrosomes). Bars (all panels) = 10 μ m.

Figure 3: Depletion of Tctex-1 results in increase cilia length. Cells were transfected with siRNA duplexes targeting each cytoplasmic dynein subunit. (A) Graph showing the mean cilia length for those subunits for which a statistically detectable difference in cilia length was found. Error bars show s.d., asterisks show p values determined from ANOVA with Dunnett's post-hoc test compared to the lamin A/C depleted control compared to lamin A/C suppressed cells (3 independent experiments). (B) Means (gray bars) and individual measurements of cilia length following suppression of lamin A/C, Tctex-1 and DHC2. (C) QPCR was used to monitor the efficacy of depletion for each DHC2 duplex used. (D) Immunoblotting shows efficiency of the depletion of Tctex-

1; lamin A/C is included as a control, GAPDH as a loading control. (E) Images of cells suppressed for lamin A/C or Tctex-1 and expressing GFP-Rab8a. Bars = 10 μ m.

Figure 4: Depletion of DHC2 results in concomitant loss of Tctex-1. Cells transfected with siRNA duplexes targeting dynein subunits as indicated were processed for immunoblotting with antibodies to detect lamin A/C, GAPDH (as a loading control) or Tctex-1 as indicated. Molecular weight markers are shown (kD). (B) Quantitation of the amount of Tctex-1 remaining. Statistical evaluation shows p values determined from ANOVA with Dunnett's post-hoc test compared to lamin A/C depleted control (3 independent experiments). Gray bars indicate those suppressions for which a statistically detectable increase in cilia length was observed (Figure 3). (C) Immunofluorescence showing acetylated tubulin labelling of cells depleted of both DHC2 and Tctex-1 with siRNA duplexes as indicated. Each box is 20 x 20 μ m.

Figure 1

Figure 1

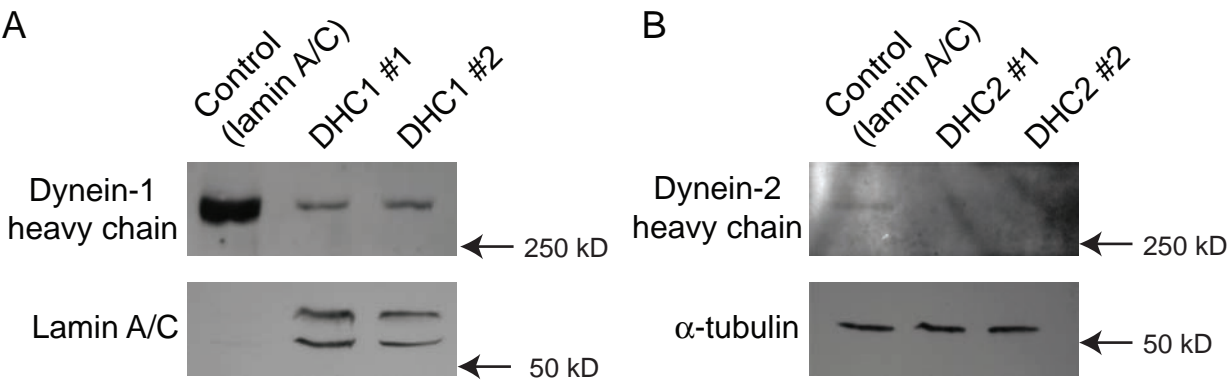


Figure 2

Figure 2

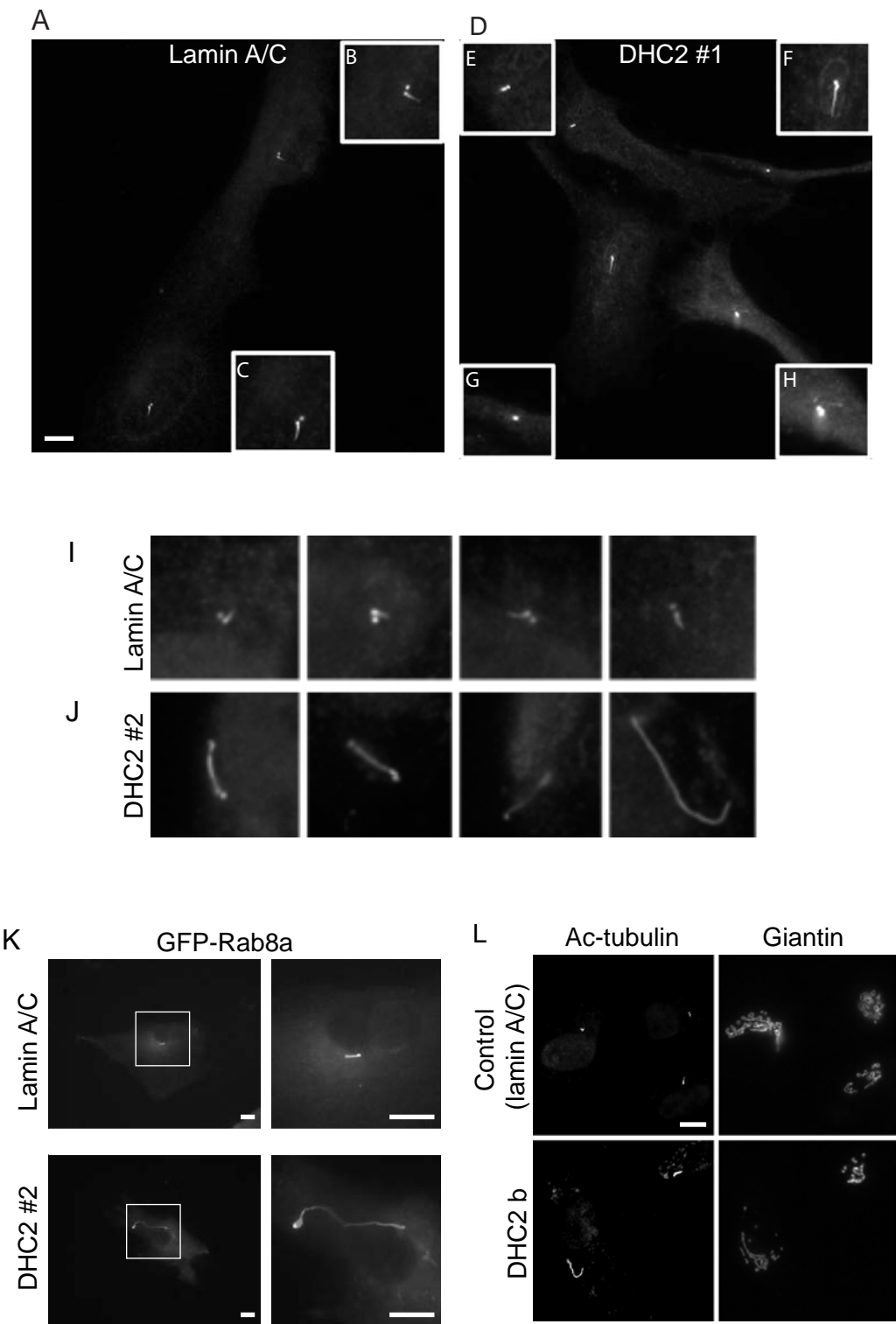


Figure 3

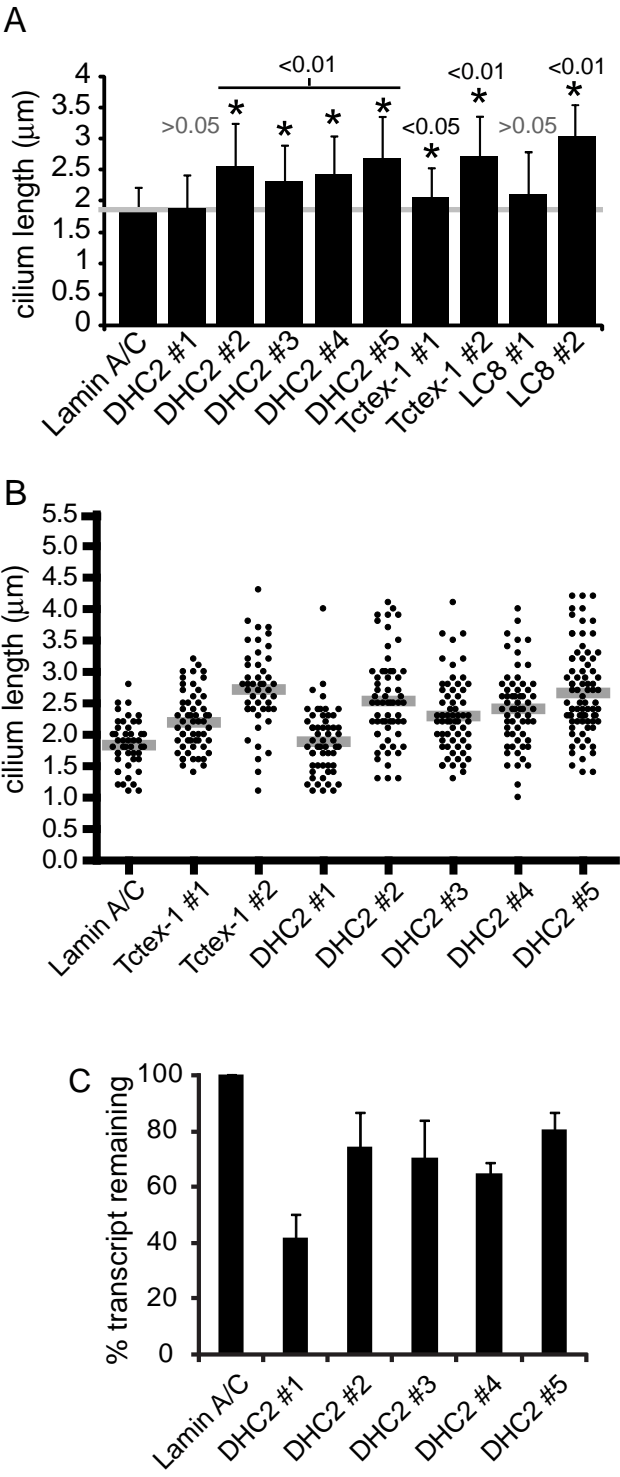


Figure 3

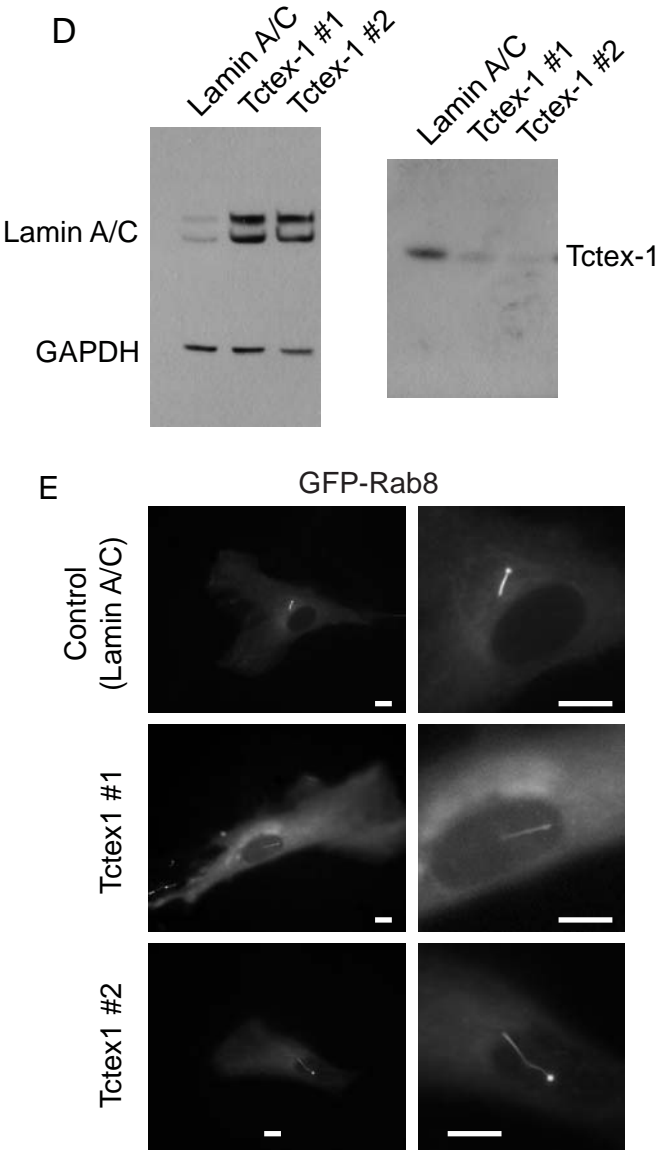


Figure 4

Figure 4

